ANTIVIRAL IMMUNITY



# PGD2/DP2 receptor activation promotes severe viral bronchiolitis by suppressing IFN-λ production

**Rhiannon B. Werder,[1] Jason P. Lynch,[1] Jennifer C. Simpson,[1,2] Vivian Zhang,[2] Nick H. Hodge,[1] Matthew Poh,[3] Elizabeth Forbes-Blom,[4] Christina Kulis,[5] Mark L. Smythe,[5] John W. Upham,[6] Kirsten Spann,[7,8] Mark L. Everard,[3] Simon Phipps[2,7]***

**Prostaglandin D2 (PGD2) signals through PGD2 receptor 2 (DP2, also known as CRTH2) on type 2 effector cells to promote asthma pathogenesis; however, little is known about its role during respiratory syncytial virus (RSV) bronchiolitis, a major risk factor for asthma development. We show that RSV infection up-regulated hematopoietic prostaglandin D synthase expression and increased PGD2 release by cultured human primary airway epithelial cells (AECs). Moreover, PGD2 production was elevated in nasopharyngeal samples from young infants hospitalized with RSV bronchiolitis compared to healthy controls. In a neonatal mouse model of severe viral bronchiolitis, DP2 antagonism decreased viral load, immunopathology, and morbidity and ablated the predisposition for subsequent asthma onset in later life. This protective response was abolished upon dual DP1/DP2 antagonism and replicated with a specific DP1 agonist. Rather than mediating an effect via type 2 inflammation, the beneficial effects of DP2 blockade or DP1 agonism were associated with increased interferon-λ (IFN-λ) [interleukin-28A/B (IL-28A/B)] expression and were lost upon IL-28A neutralization. In RSV-infected AEC cultures, DP1 activation up-regulated IFN-λ production, which, in turn, increased IFN-stimulated gene expression, accelerating viral clearance. Our findings suggest that DP2 antagonists or DP1 agonists may be useful antivirals for the treatment of viral bronchiolitis and possibly as primary preventatives for asthma.**

## INTRODUCTION

Asthma is characterized by airway remodeling, airway hyperreactivity, and most typically type 2 inflammation, orchestrated by $CD4^+$ T helper 2 ($T_H2$) cells and type 2 innate lymphoid cells (ILC2) (*1*). These two cell types are the primary producers of type 2 cytokines [interleukin-5 (IL-5) and IL-13], which can induce the pathophysiological features of asthma, either via the direct activation of stromal cells or indirectly via the stimulation of key effector cells, such as eosinophils and mast cells. Consequently, upstream activators of $T_H2$ cells and ILC2s are now a major focus of research efforts (*2*). The eicosanoid prostaglandin D2 (PGD2), long recognized as a potent bronchoconstrictor (*3*, *4*), is now recognized to act as a chemoattractant and inducer of type 2 cytokine production by $T_H2$ cells and ILC2s (*5*, *6*). As a consequence, the PGD2-responsive G protein–coupled receptors DP1 and DP2 [also known as chemoattractant receptor–homologous molecule expressed on $T_H2$ lymphocytes (CRTH2)] and the enzyme hematopoietic prostaglandin D synthase (h-PGDS) have all emerged as tractable drug targets in the treatment of allergic disease (*7*).

The role of DP1 in asthma pathogenesis remains contentious. DP1 activation was observed to promote $CD4^+$ $T_H2$ cell differentiation in vitro (*8*); however, in preclinical models of asthma, DP1 agonism attenuates type 2 inflammation by suppressing dendritic cell (DC) migration, maturation, and differentiation and expanding peripheral regulatory T cells (*9*). In contrast, small-molecule DP2 antagonists diminish the magnitude of allergic inflammation in acute and chronic animal models, decreasing cellular recruitment and arresting $T_H2$ cytokine production (*10*, *11*). These experimental findings were predictive of clinical efficacy, because various clinical trials with different DP2 antagonists have since demonstrated improved lung function and attenuated $T_H2$ responses in patients with allergic asthma (*12*, *13*). In contrast, treatment with a dual DP1-DP2 antagonist did not improve asthma symptoms or lung function (*14*).

Lower respiratory viral infections are associated with the onset, progression, and acute exacerbations of asthma. Severe respiratory syncytial virus (RSV) or rhinovirus-induced bronchiolitis, and/or frequent viral-induced wheezing in infancy are major independent risk factors for the development of childhood asthma (*15*, *16*). Notably, this risk is markedly increased (up to 30-fold) in infants who become sensitized to allergens (*17*, *18*). This interplay between virus infections and allergen exposures, together with genetic risk factors, most likely dysregulates antiviral immunity and induces a microenvironment in the airway mucosa that favors the development of $T_H2$ immunity. Notably, both type 2 "initiating" (for example, IL-33) and "effector" (for example, IL-4) cytokines negatively regulate the production of antiviral cytokines including type I (α/β) and type III (λ) interferons (IFNs) (*19*–*21*), and thus, the development of aberrant type 2 immune responses in infancy may adversely affect host susceptibility to subsequent infections in childhood and later life. Accordingly, a better understanding of the pathogenic mechanisms by which RSV infection induces $T_H2$ immunity and severe bronchiolitis may yield new opportunities for therapeutic intervention and potentially primary prevention for allergic asthma (*22*). Despite its role as an inducer of $T_H2$ immunity, the contribution of PGD2 to the pathogenesis of RSV bronchiolitis has yet to be explored. Here, we tested the hypothesis that the production of PGD2 is elevated during viral

[1]School of Biomedical Sciences, University of Queensland, Queensland 4072, Australia. [2]Queensland Institute of Medical Research Berghofer Medical Research Institute, Herston 4006, Australia. [3]School of Paediatrics and Child Health, University of Western Australia, Western Australia 6840, Australia. [4]Malaghan Institute of Medical Research, Wellington 6242, New Zealand. [5]Institute for Molecular Bioscience, University of Queensland, Queensland 4072, Australia. [6]Diamantina Institute, University of Queensland, Translational Research Institute, Princess Alexandra Hospital, Queensland 4102, Australia. [7]Australian Infectious Diseases Research Centre, University of Queensland, Queensland 4067, Australia. [8]School of Biomedical Sciences, Queensland University of Technology, Queensland 4001, Australia.
*Corresponding author. Email: simon.phipps@qimrberghofer.edu.au

bronchiolitis and contributes to disease severity by promoting type 2 inflammation and suppressing antiviral immunity via the activation of DP2.

## RESULTS

### Severe pneumovirus bronchiolitis up-regulates h-PGDS and PGD2

We previously developed a preclinical model of viral bronchiolitis and subsequent chronic asthma by inoculating mice in infancy ("bronchiolitis phase") and adolescence ("progression to asthma phase") with pneumonia virus of mice (PVM; the murine analog of RSV) and low-dose cockroach allergen (CRE) (*19*). To explore whether virus infection and/or exposure to CRE affected the production of PGD2 during the bronchiolitis phase (Fig. 1A), we first measured the expression of cytoplasmic h-PGDS, because this isoform of PGDS is expressed by leukocytes and lung stromal cells (*23*, *24*). In vehicle-exposed neonatal mice, leukocyte numbers in the lung were sparse, and consequently, basal h-PGDS was predominantly expressed, albeit weakly, in bronchial airway epithelial cells (AECs; Fig. 1, B to D, and fig. S1A). After PVM inoculation, h-PGDS increased only in the airway epithelium (not the hematopoietic cells) and did not occur until 10 days post infection (dpi; Fig. 1, B and D, and fig. S1A). In contrast, CRE exposure of either PVM-infected or noninfected mice induced a significant increase in h-PGDS$^+$ inflammatory cells within 2 hours (that is, at 3 dpi$^{+2hr}$; $P < 0.001$; Fig. 1B and fig. S1A), although the response waned within 48 hours. In contrast to PVM infection, CRE exposure alone did not affect h-PGDS expression in AECs, whereas in PVM-infected mice, CRE exposure significantly increased h-PGDS expression in AECs at 7 and 10 dpi compared to mice exposed to PVM alone, CRE alone, or vehicle ($P < 0.001$; Fig. 1, C and D).

Having previously identified an important role for IL-33 in this model (*19*), we next questioned whether IL-33 regulates h-PGDS expression in AECs. Whereas exposure to low-dose exogenous IL-33 from 3 to 5 dpi had no effect on h-PGDS expression, PVM/IL-33 coexposure (study design shown in fig. S1B) increased the number of h-PGDS$^+$ AECs at 7 dpi (Fig. 1E). In addition, anti–IL-33 treatment of PVM/CRE-coexposed mice significantly decreased epithelial h-PGDS expression at 7 and 10 dpi ($P < 0.01$ and $P < 0.001$; fig. S1C). Consistent with the distinct cellular and biphasic expression of h-PGDS in the airway mucosa, PGD2 production in the airway peaked at 5 and 10 dpi and was elevated in PVM/CRE-coexposed mice (but not in PVM-alone or CRE-alone control groups) when compared to vehicle-exposed mice (Fig. 1F).

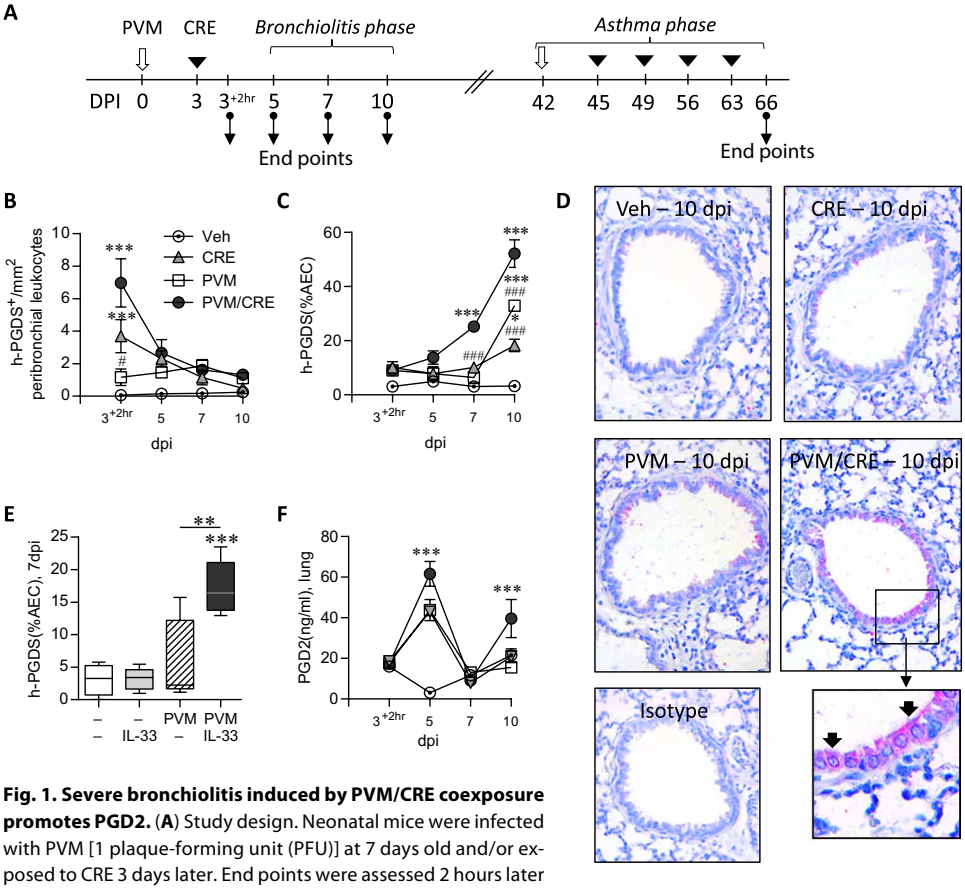


**Fig. 1. Severe bronchiolitis induced by PVM/CRE coexposure promotes PGD2.** (**A**) Study design. Neonatal mice were infected with PVM [1 plaque-forming unit (PFU)] at 7 days old and/or exposed to CRE 3 days later. End points were assessed 2 hours later at 5, 7, or 10 dpi. To induce asthma-like pathology, mice were reinfected with PVM and exposed to CRE as shown, and end points were assessed at 66 dpi. h-PGDS expression in (**B**) peribronchial leukocytes or in (**C** and **D**) AECs (arrows indicate positive AECs), analyzed by two-way analysis of variance (ANOVA). (**E**) Neonates were infected with PVM and/or treated with low-dose exogenous IL-33. h-PGDS in AECs was assessed at 7 dpi. (**F**) PGD2 in the lung. Data are presented as mean ± SEM or as box-and-whisker plots to show quartiles (boxes) and range (whiskers) and are representative of two experiments ($n$ = 5 to 8 mice per group per experiment), analyzed by one-way ANOVA. *$P < 0.05$, **$P < 0.01$, and ***$P < 0.001$ compared with vehicle-treated mice. $^{\#}P < 0.05$ and $^{\#\#\#}P < 0.001$ compared with PVM/CRE mice.

### RSV infection up-regulates h-PGDS and PGD2

We sought to validate our experimental mouse studies using ex vivo cultures of primary bronchial human (h)AECs obtained from healthy children. Similar to our findings in mice, and consistent with a previous report (*25*), basal h-PGDS and PGD2 production were detectable in the absence of infection (Fig. 2, A to C), and mirroring our in vivo findings with PVM, infection with RSV [multiplicity of infection (MOI), 1] led to a substantial increase in h-PGDS expression and PGD2 production at 24 and 48 hours (Fig. 2, A to C). This observation led us to question whether PGD2 production is elevated in the upper airways of children with severe RSV bronchiolitis. Compared to healthy infant controls, nasal secretions obtained from young infants with severe RSV bronchiolitis (mean age, 16 weeks; Fig. 2D) contained significantly higher levels of PGD2, implicating a role for PGD2 in disease pathogenesis ($P < 0.05$; Fig. 2E).

### DP2 antagonism promotes viral clearance and antiviral cytokine production

To explore the contribution of PGD2 to severe viral bronchiolitis, we returned to the preclinical model and treated mice

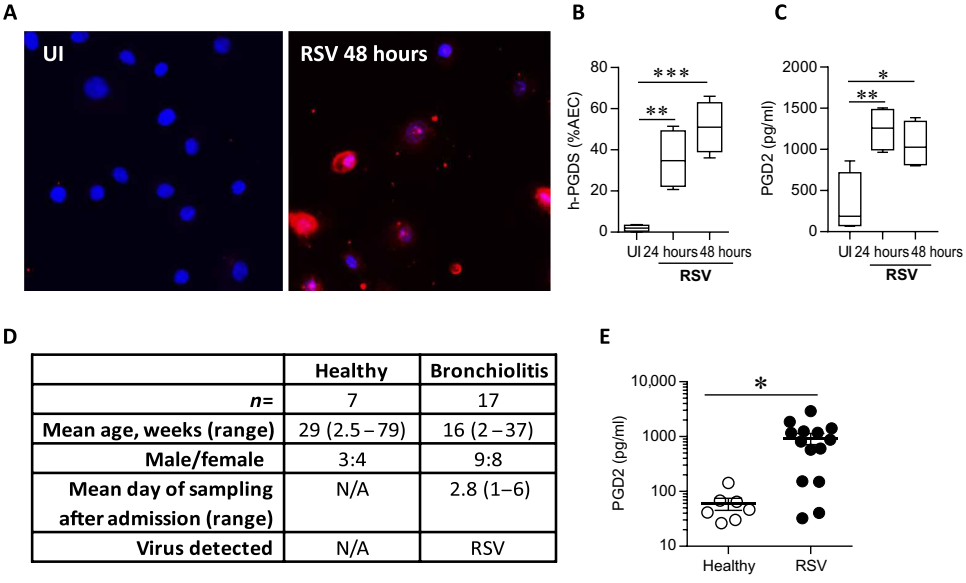


D

| | Healthy | Bronchiolitis |
|---|---|---|
| *n*= | 7 | 17 |
| Mean age, weeks (range) | 29 (2.5 – 79) | 16 (2 – 37) |
| Male/female | 3:4 | 9:8 |
| Mean day of sampling after admission (range) | N/A | 2.8 (1–6) |
| Virus detected | N/A | RSV |




**Fig. 2. RSV infection promotes PGD2.** Pediatric human bronchial epithelial cells isolated from healthy children were uninfected (UI) or infected with RSV (MOI, 1). (**A**) h-PGDS (red) and nuclei (blue) in uninfected (left) or 48 hours after RSV infection (right) in hAECs. (**B**) h-PGDS expression was quantified as a percentage of hAECs. (**C**) PGD2 was detected in cell supernatants. Box-and-whisker plots show quartiles (boxes) and range (whiskers), and data are representative of three experiments ($n = 4$ individual hAEC samples per group in duplicate), analyzed by one-way ANOVA. (**D**) Details of bronchiolitis patients. (**E**) Nasal swabs were collected from healthy infants or those admitted to the hospital with RSV bronchiolitis, and PGD2 was measured. $n = 7$ to 14 infants per group, analyzed by Mann-Whitney test. *$P < 0.05$, **$P < 0.01$, and ***$P < 0.001$.

with the DP2 antagonist AM156 ({2′-[(cyclopropanecarbonyl-ethyl-amino)-methyl]-6-methoxy-4′-trifluoro-methyl-biphenyl-3-yl}-acetic acid) (daily oral gavage, 10 mg/kg) from 3 to 9 dpi (Fig. 3A). Consistent with our previous report (*19*), PVM/CRE-coexposed mice developed severe bronchiolitis that was associated with stunted weight gain (a phenotype that does not occur in PVM-alone or CRE-alone mice) and increased viral load in the airway epithelium and whole lung (Fig. 3, B to D). In response to AM156 treatment, there was a significant improvement in weight gain ($P < 0.001$) and a diminution of viral load when assessed in the airway epithelium or whole lung (Fig. 3, B to D). DP2 antagonism did not affect viral load in mice infected with PVM alone.

Having previously established that CRE exposure of PVM-infected mice delays viral clearance by impairing the production of IFN-α and IFN-λ [specifically IL-28A and/or IL-28B; the enzyme-linked immunosorbent assay (ELISA) detects both proteins] in the BALF and IL-12p40 in the lungs (*19*), we next assessed the effect of DP2 antagonism on the production of these cytokines. Compared to the PVM infection–alone group, PVM/CRE-coexposed mice produced similar amounts of IFN-γ but markedly less IFN-α, IFN-λ, and IL-12p40 protein; strikingly, all three cytokines were substantially elevated at 7 dpi after treatment with AM156 (Fig. 3E, bottom). This response was not associated with an increase in natural killer cell, $CD8^+$ T cell, or plasmacytoid DC numbers (fig. S2, A to C), the latter being lower in coexposed mice treated with AM156. At 5 dpi, IFN-α or IL-12p40 concentrations were not dampened in coexposed mice and therefore unaffected by AM156. By contrast, DP2 antagonism restored IFN-λ concentrations (Fig. 3E, top), implicating a key role for this cytokine in controlling viral load in the early-phase response (Fig. 3, C to D). Consistent with the pattern of IFN production, the attenuated expression of the IFN-stimulated gene (ISG) *Irf7* in PVM/CRE-coexposed mice was reversed at 5 and 7 dpi after DP2 antagonism (Fig. 3F). One mechanism by which IFNs counter viral infections is via the induction of apoptosis (*26*). We observed that the gene expression of *Caspase-3* (*Casp3*), the effector caspase of apoptosis, was lower in PVM/CRE-coexposed mice. Conversely, treatment with AM156 reversed this phenotype, enhancing *Casp3* expression at 5 and 7 dpi (Fig. 3G).

We next investigated whether the beneficial effects of DP2 antagonism at 5 dpi were dependent on IFN-λ signaling by neutralizing IL-28A (also known as IFN-λ2; Fig. 3H). Critically, anti–IL-28A treatment abrogated the AM156-induced reduction in viral load and prevented the up-regulation in *Irf7* and *Casp3* expression (Fig. 3, I to L).

## DP2 antagonism prevents type 2 inflammation and ASM growth

Several studies have reported increased features of type 2 inflammation in young children infected with RSV (*27*, *28*), a phenotype that is replicated and most pronounced at 10 dpi in PVM/CRE-coexposed mice (fig. S3A) and that does not occur with PVM infection alone (*19*). When we compared PVM/CRE-coexposed mice treated with and without AM156, we found that DP2 antagonism significantly decreased the numbers of lung ILC2s and airway eosinophils ($P < 0.05$), as well as airway neutrophils, lymphocytes, and mononuclear cells (Fig. 4, A and B, and fig. S3, B to D). This response was associated with a decrease in PGD2 but not in IL-33 concentration (Fig. 4, C to D), which we had previously shown to be elevated at 3 and 10 dpi (*19*). Consistent with a lack of PGD2 production in CRE-alone or PVM-alone mice, DP2 antagonism had no effect on eosinophilia or ILC2 numbers in the lung in these groups (fig. S3, E and F). To assess the direct effect of DP2 antagonism on ILC2 function, we FACS (fluorescence-activated cell sorter)-purified ILC2s from PVM/CRE-coexposed mice. As expected, DP2 antagonism attenuated the production of IL-5 and IL-13 by ILC2s in response to IL-2/PGD2 (Fig. 4, E and F). Exogenous IFN-λ (IL-28A) was also able to substantially decrease the production of both type 2 cytokines (Fig. 4, E and F), without affecting ILC2 proliferation or apoptosis (fig. S4, A and B).

Because type 2 cytokines can suppress type I and type III IFN production (*20*, *29*) and DP2 antagonism decreased lung ILC2s (Fig. 4A), it was possible that the type 2 inflammation in coexposed mice acted upstream of the suppressive effects of PGD2/DP2 agonism on IFN-λ expression. Although the expression of IL-4 and IL-13 was not elevated until 10 dpi (fig. S3A), 5 days after the dampened IFN-λ response (Fig. 3E), we attempted to further exclude a role for IL-13 by treating PVM/CRE-coexposed mice with soluble IL-13Rα2 fusion protein (fig. S4C). As expected, blockade of IL-13 signaling had no effect on viral load, IFN-λ expression, or downstream *Irf7* or *Casp3* expression (fig. S4, D to H).

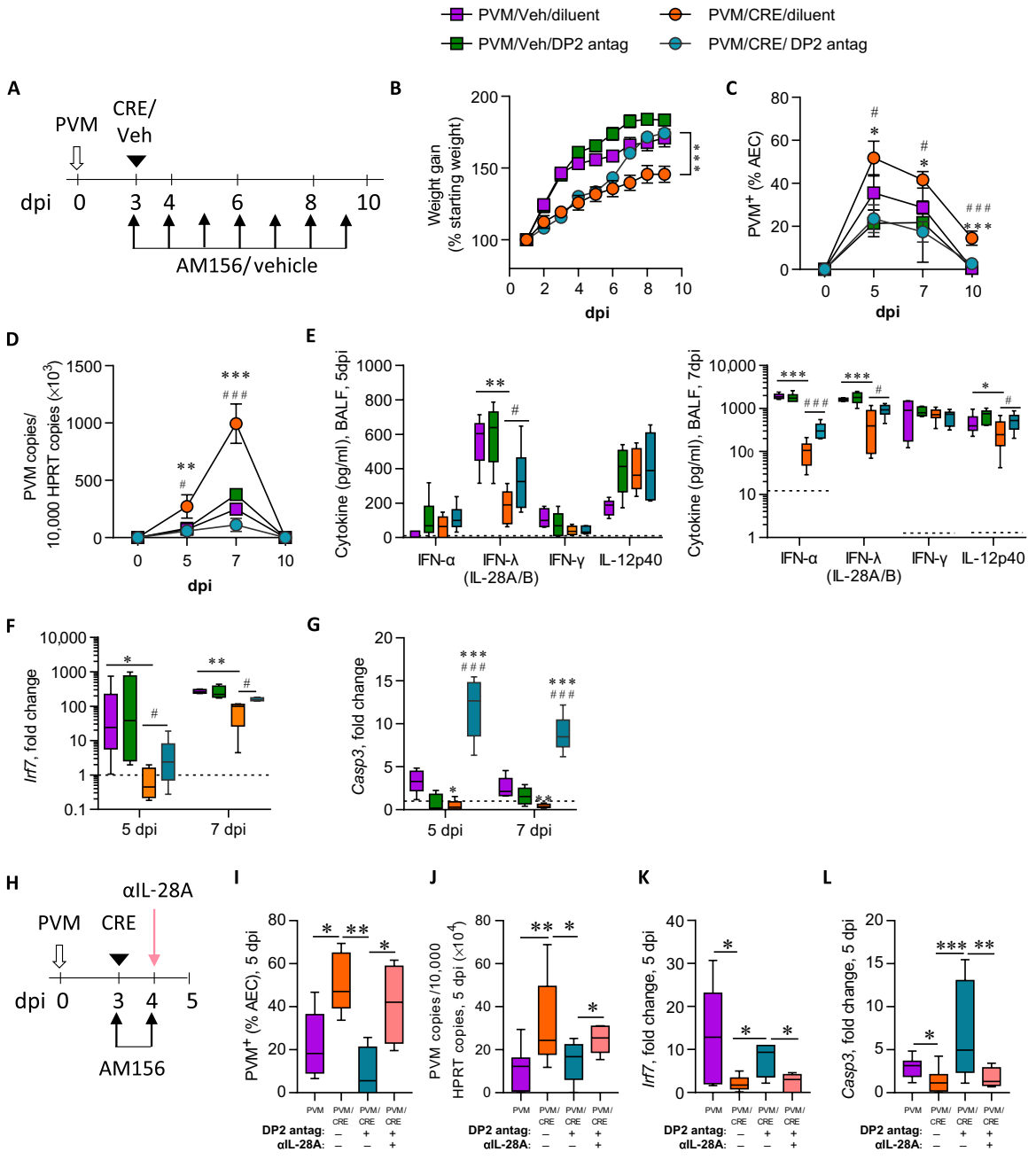


**Fig. 3. DP2 antagonism promotes antiviral immunity in PVM/CRE mice.** (**A**) Study design. Mice were inoculated at 7 days old with PVM and then exposed to CRE 3 dpi (intranasal). Some mice were treated daily with a DP2 antagonist (AM156) from 3 to 9 dpi (oral gavage). End points were assessed at 5, 7, and 10 dpi. (**B**) Weight gain. (**C**) Viral load in AECs detected by immunohistochemistry, or (**D**) whole-lung viral copies assessed by quantitative polymerase chain reaction (qPCR). (**E**) IFN-α, IFN-λ (IL-28A/B), and IFN-γ expression in bronchoalveolar lavage fluid (BALF) and IL-12p40 expression in lung were assessed at 5 dpi (top) and 7 dpi (bottom). (**F**) *Interferon regulatory factor 7* (*Irf7*) gene and (**G**) Caspase-3 (*Casp3*) gene expression in whole lung was assessed by qPCR. (**H**) Mice were inoculated with PVM ± CRE and treated daily with AM156. Some mice were treated with anti–IL-28A (intraperitoneally) at 4 dpi. (**I**) Viral load in AECs or (**J**) viral copies. (**K**) *Irf7* and (**L**) *Casp3* expression. Data are presented as mean ± SEM or as box-and-whisker plots to show quartiles (boxes) and range (whiskers) and are representative of two experiments ($n = 5$ to 10 mice per group), analyzed by one-way or two-way ANOVA. $^{*}P < 0.05$, $^{**}P < 0.01$, and $^{***}P < 0.001$ compared with PVM-alone mice or as indicated. $^{\#}P < 0.05$ and $^{\#\#\#}P < 0.001$ compared with PVM/CRE mice. Dashed lines represent uninfected controls.

In addition to the attenuated type 2 inflammation in vivo, DP2 antagonism prevented smooth muscle growth around the small airways (Fig. 4G), a cardinal feature of asthma that is now recognized to commence in early life before asthma diagnosis (*30*). To assess whether PGD2 acts directly to induce ASM growth, we isolated and cultured mouse primary tracheal ASM cells in the presence of various concentrations of PGD2. Using a fluorescence-based proliferation assay, we found that PGD2 was a potent ASM cell mitogen, with an $EC_{50}$ (median effective concentration) of ~1 pg/ml (Fig. 4H). Although DP1 and DP2 gene expression was similar on the ASM cells (fig. S4I), DP2-specific

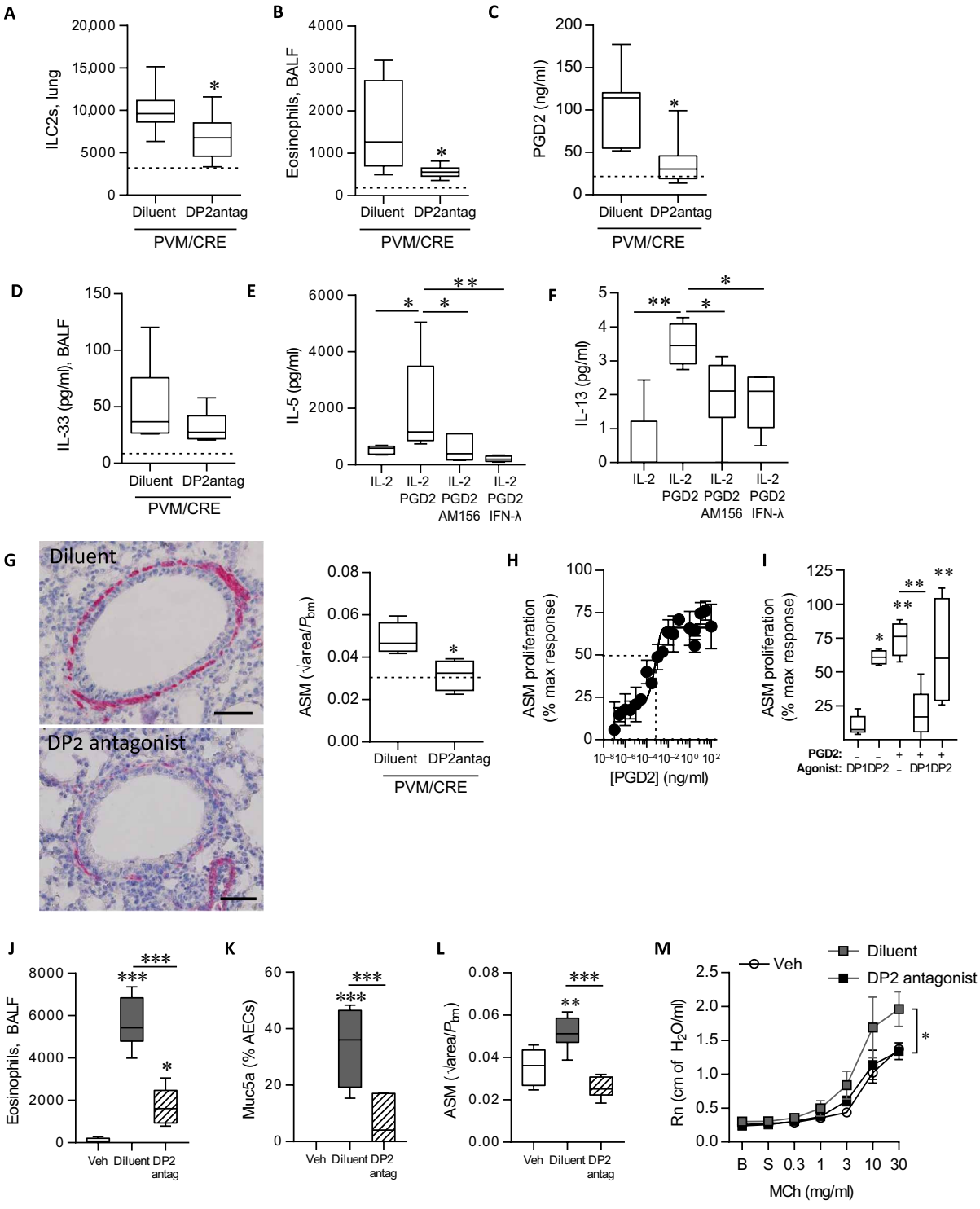


**Fig. 4. DP2 antagonism ameliorates type 2 inflammation in PVM/CRE mice.** Mice were treated as per Fig. 3A. (**A**) ILC2s in the lung. (**B**) Eosinophils in the BALF. (**C**) PGD2 expression in the lung and (**D**) IL-33 expression in the BALF. ILC2s were isolated from PVM/CRE mice and cultured with PGD2 ± DP2 antagonist (AM156) or IFN-λ. (**E**) IL-5 and (**F**) IL-13 expression was measured in the supernatant. (**G**) Airway smooth muscle (ASM) mass in vivo expressed as √area/perimeter of the basement membrane ($P_{bm}$). (**H**) ASM cells were isolated and cultured from neonatal mice and stimulated, and proliferation was measured using V450 dye dilution. Data are presented as mean ± SEM. (**I**) ASM cells were stimulated with PGD2, DP1-specific, or DP2-specific agonists, and proliferation was measured. (**J**) PVM/CRE-infected mice were treated with the DP2 antagonist as per Fig. 3A and then exposed to PVM and CRE in later life (as per Fig. 1A) to induce asthma-like pathologies. Eosinophils in the BALF. (**K**) Muc5a expression as a percentage of AECs. (**L**) ASM mass. (**M**) Airway resistance (Rn) in response to increasing doses of methacholine (MCh). Data are presented as mean ± SEM or as box-and-whisker plots to show quartiles (boxes) and range (whiskers) and are representative of two experiments ($n = 4$ to 8 mice per group or four to five replicates in vitro), analyzed by Mann-Whitney test or one-way or two-way ANOVA. *$P < 0.05$, **$P < 0.01$, and ***$P < 0.001$. Dashed lines represent uninfected controls.

agonism (with 15*R*-methyl-PGD2; 4 nM) but not DP1-specific agonism (with BW245C; 60 nM) induced ASM cell proliferation. The DP1-specific agonist significantly decreased exogenous PGD2-induced ASM cell proliferation ($P < 0.01$), indicating that DP1 and DP2 activation elicit opposing responses (Fig. 4I). Collectively, these results demonstrate a critical role for PGD2-DP2 signaling in inducing ASM growth both in vivo and in vitro. We next examined whether the protective effect of DP2 antagonism against severe bronchiolitis in infancy would decrease susceptibility to the development of asthma-like pathologies in later life (see study design in Fig. 1A) (*19*). Strikingly, DP2 antagonism in early life alone was sufficient to attenuate the development of secondary PVM and CRE exposure–induced chronic asthma as shown by the reduced airway eosinophils, mucus hypersecretion, ASM mass, and airways hyperreactivity (Fig. 4, J to M). The effect of DP2 antagonism was not assessed in PVM/PVM- or CRE/CRE-exposed mice because these mice do not develop an asthma-like pathology (*19*).

### DP2 but not DP1 antagonism ameliorates bronchiolitis

DP1 activation is protective in an acute model of allergic asthma (*9*) and inhibited PGD2-induced ASM cell proliferation in our in vitro model, leading us to hypothesize that DP1 activation contributes to the beneficial effects induced by DP2 antagonism. To investigate this, we treated the PVM/CRE-coexposed mice with a DP1 antagonist (MK-0524), a DP2 antagonist (AM156), or both antagonists simultaneously (Fig. 5A). In contrast to DP2 antagonism, DP1 antagonism had no effect on viral load when assessed in the airway epithelium or whole lung (Fig. 5, B and C). However, DP1 antagonism ablated the beneficial effects of DP2 antagonism on viral clearance (Fig. 5, B and C). Consistent with an important role for DP1 agonism in promoting antiviral immunity in the wake of DP2 antagonism, dual DP1/DP2 antagonism prevented the restorative effects of DP2 antagonism on IFN-α, IFN-λ, and IL-12p40 concentrations in BALF (Fig. 5D and fig. S5, A to C) and ISG expression in the lung (Fig. 5, E to F). Similarly, in the context of type 2 inflammation, DP1 antagonism alone was without effect, and dual DP1/DP2 antagonism ablated the beneficial effects of AM156 on airway eosinophils, lung ILC2s, and ASM growth (Fig. 5, G to I).

### DP1 activation promotes antiviral immunity in vivo

To directly assess the contribution of DP1 and DP2 agonism, we next treated PVM-infected mice with a specific DP1 (BW245C; 1 mg/kg)

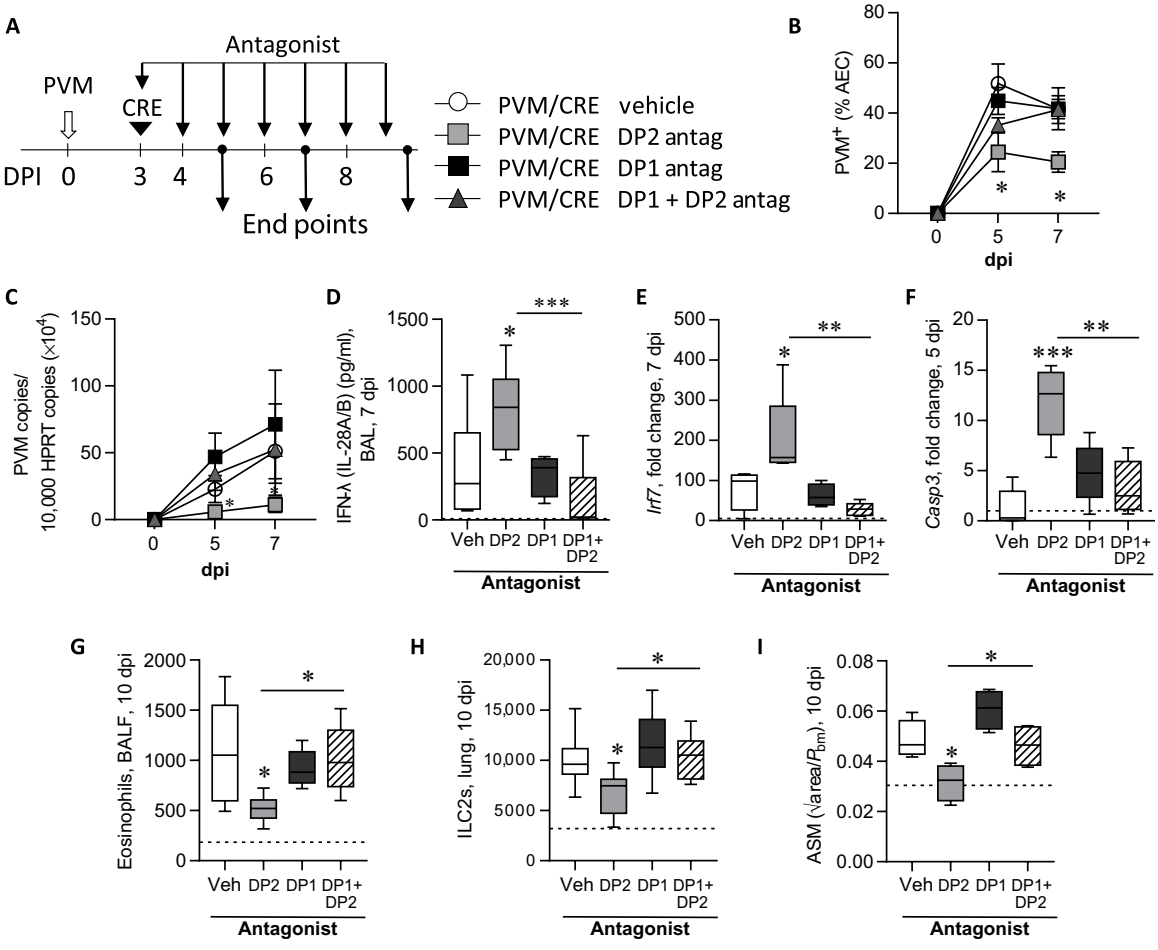


**Fig. 5. DP2 but not DP1 antagonism prevents severe bronchiolitis in PVM/CRE mice.** (**A**) Study design. Mice were inoculated at 7 days old with PVM and then exposed to CRE 3 dpi (intranasal). Some mice were treated daily from 3 dpi with a DP2 antagonist (AM156), a DP1 antagonist (MK-0524), or both antagonists from 3 to 9 dpi (oral gavage). End points were assessed at 5, 7, and 10 dpi. (**B**) Viral load in AECs detected by immunohistochemistry or (**C**) whole-lung viral copies assessed by qPCR. (**D**) IFN-λ (IL-28A/B) expression in the BALF at 7 dpi. (**E**) *Irf7* and (**F**) *Casp3* gene expression in whole lung assessed by qPCR. (**G**) Eosinophils in the BALF at 10 dpi. (**H**) ILC2s in the lung at 10 dpi. (**I**) ASM mass expressed as √area/perimeter of the basement membrane at 10 dpi ($P_{bm}$). Data are presented as mean ± SEM or as box-and-whisker plots to show quartiles (boxes) and range (whiskers) and are representative of two experiments ($n$ = 4 to 8 mice per group), analyzed by one-way or two-way ANOVA. *$P < 0.05$, **$P < 0.01$, and ***$P < 0.001$. Dashed lines represent uninfected controls.

or DP2 (15*R*-methyl-PGD2; 1 mg/kg) agonist and compared the response to PVM-infected mice inoculated with CRE, exogenous PGD2 (5 μg/kg), or diluent control (Fig. 6A). DP1 agonism massively decreased viral load in the airway epithelium, whereas exogenous PGD2 or DP2 agonism delayed viral clearance (similar to PVM/CRE-coexposed mice; Fig. 6, B and C). Similar to our observations with DP2 antagonism, DP1 agonism increased the expression of IFN-λ protein, up-regulated *Irf7* and *Casp3* gene expression, and promoted AEC expression of cleaved caspase-3 (Fig. 6, D to G). Notably, IL-12p40 and IFN-α concentrations were not affected by DP1 agonism (fig. S6, A to C), inferring a primary

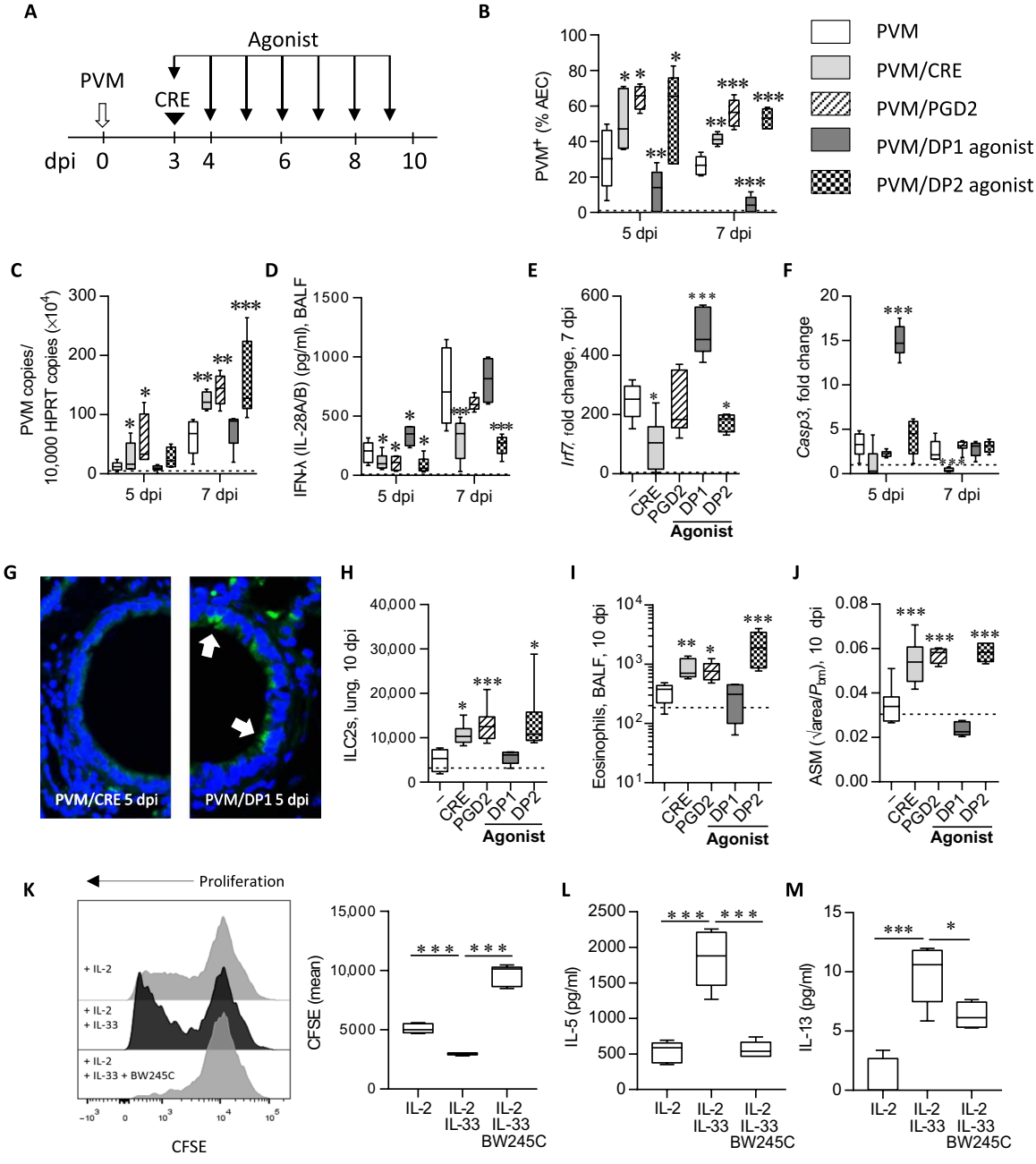


**Fig. 6. DP1 activation promotes IFN-λ to limit viral load and type 2 inflammation.** (**A**) Study design. All mice were inoculated at 7 days old with PVM. PVM/CRE-coexposed mice were exposed to CRE at 3 dpi and received no other treatment. Mice that received PGD2, a DP1 agonist (BW245C), or a DP2 agonist [15(*R*)-15-methyl-PGD2] were treated daily from 3 to 9 dpi. End points were assessed at 5, 7, and 10 dpi. (**B**) Viral load in AECs detected by immunohistochemistry or (**C**) whole-lung viral copies assessed by qPCR. (**D**) IFN-λ (IL-28A/B) expression in the BALF at 5 and 7 dpi. (**E**) *Irf7* gene and (**F**) *Casp3* gene expression in whole lung assessed by qPCR. (**G**) Cleaved caspase-3 expression (green) and nuclei (blue). (**H**) ILC2s in the lung at 10 dpi. (**I**) Eosinophils in the BALF at 10 dpi. (**J**) ASM mass expressed as √area/perimeter of the basement membrane at 10 dpi. (**K**) ILC2s were cultured with IL-33 ± DP1 agonist (BW245C). ILC2 proliferation was measured by dilution of carboxyfluorescein diacetate succinimidyl ester (CFSE). (**L**) IL-5 and (**M**) IL-13 secretion measured in the supernatant. Box-and-whisker plots show quartiles (boxes) and range (whiskers), and data are representative of two experiments ($n$ = 4 to 8 mice per group or five replicates in vitro), analyzed by one-way or two-way ANOVA. *$P$ < 0.05, **$P$ < 0.01, and ***$P$ < 0.001 compared to PVM-alone mice or as indicated. Dashed lines represent uninfected controls.

role for IFN-λ in accelerating viral clearance. In the absence of infection, DP1 agonism had no effect on IFN-λ production. In the context of type 2 inflammation, exposure of PVM-infected mice to exogenous PGD2 or the DP2 agonist increased lung ILC2s, airway eosinophils, and ASM growth, similar to the effects of PVM/CRE exposure (Fig. 6, H to J). By contrast, treatment of infected mice with the DP1 agonist did not promote type 2 inflammation or ASM remodeling. Despite the increase in type 2 inflammation, neither exogenous PGD2 nor the DP2 agonist increased IL-33 at 10 dpi, consistent with the notion that IL-33 is upstream of PGD2.

A role for DP1 agonism in decreasing lung ILC2s was implicated by the lack of benefit after dual DP1/DP2 antagonism as compared to DP2 antagonism (Fig. 5); however, it remained unclear whether this effect was mediated directly or indirectly (for example, via increased IFN-λ expression), or both. To address this, we FACS-purified ILC2s from PVM/CRE-coexposed mice and stimulated the cells with IL-2 and IL-33 for 3 days in the absence or presence of the DP1 agonist BW245C. DP1 agonism attenuated IL-2/IL-33–induced proliferation and type 2 cytokine production by ILC2s (Fig. 6, K to M), suggesting that DP1 activation can act directly to dampen these potent type 2 effector cells.

### DP1 activation promotes antiviral immunity in ex vivo–cultured AECs via type III IFN

Our in vivo findings obtained with the DP1/DP2-specific agonists and antagonists suggested that DP2 antagonism promoted antiviral immunity by enhancing the production of IFN-λ. Because AECs preferentially express the type III IFN receptor and are a rich source of the IFN-λ family of cytokines (encoded by *IL28A*, *IL28B*, and *IL29*) (*31*), we returned to the primary hAEC culture model to test this theory. Strikingly, DP2 antagonism significantly reduced viral burden at 24 and 48 hours after RSV infection ($P < 0.05$; Fig. 7A). This was coupled with a boost in IFN-λ (IL-28A) gene and protein expression (Fig. 7, B and C; note that the ELISA for human IFN-λ is specific for IL-28A) and the downstream up-regulation of *IRF7* and *CASP3* expression (Fig. 7, D and E). Similar to our in vivo experiments, we confirmed that this effect was not influenced by type 2 cytokine production by neutralizing IL-4 and IL-13. Compared with RSV infection alone, viral load, *IL28A*, and *IRF7* were not significantly altered in the presence of anti–IL-4/IL-13 (fig. S7, A to C).

On the basis of our in vivo studies, we hypothesized that the beneficial effect of DP2 antagonism in the hAEC model was mediated via a shift to DP1 activation. Treatment with the DP1 agonist BW 245C 30 min before RSV infection substantially decreased viral load in hAECs at 24 and 48 hours (Fig. 7F). Notably, DP1 agonism in the absence of infection did not induce the expression of either *IL28A* or *IRF7* (fig. S7, D and E). In contrast to DP1 agonism, the specific DP2 agonist, 15*R*-methyl-PGD2, had no effect on viral load (fig. S7, F to H). This suggested that RSV-induced PGD2 production preferentially activates DP2, an effect that did not relate to a difference in receptor gene expression (fig. S7I). When we repeated this experiment using primary mAECs, which require differentiation at the air-liquid interface for PVM infection, DP1 agonism led to a significant decrease in viral copy number at 24 and 48 hours ($P < 0.05$; Fig. 7G), and qualitatively, fewer AECs were immunoreactive for the PVM G protein (Fig. 7H), a phenocopy of the response observed in hAEC. In both hAECs and mAECs, the lower viral load was associated with higher levels of *IL-28A* gene and IFN-λ protein expression and the downstream induction of *IRF7* and *CASP3* gene expression (Fig. 7, I to L).

To implicate IL-28A as the effector cytokine of DP1-mediated protection, we next treated the hAECs with anti–IL-28A. Neutralization of IL-28A completely ablated the antiviral effects induced by DP1 activation, leading to increased viral load and preventing the up-regulation of *IRF7* and *CASP3* at 48 hours (Fig. 8, A to C). Finally, to explore whether DP1 agonism might act more broadly and promote antiviral immunity to other viruses, we stimulated the hAECs with the Toll-like receptor 3 and RIG-I ligand polyinosinic:polycytidylic acid (polyI:C) in the absence or presence of BW 245C. Critically, DP1 activation enhanced polyI:C-induced IFN-λ gene expression at 24 hours, prolonged *IRF7* and *CASP3* gene expression, and increased IFN-λ protein expression at 48 hours (Fig. 8, D to G).

## DISCUSSION

Globally, RSV bronchiolitis is estimated to cause up to 200,000 deaths per annum. At present, there is no effective vaccine, and treatment is primarily supportive. Severe bronchiolitis is often associated with heightened viral load (*32*, *33*), which may be linked to RSV's ability to impair host IFN-λ production (*34*, *35*) or single-nucleotide polymorphisms in genes that contribute to innate antiviral immunity (*36*, *37*). Here, we identified that PGD2 concentrations are elevated in the upper airways of infants hospitalized with RSV bronchiolitis and that PGD2/DP2 activation suppresses the production of epithelial-derived IFN-λ production, thus contributing to disease pathogenesis. However, activation of the DP1 receptor elicited the opposite response, markedly increasing the production of IFN-λ, to promote antiviral immunity and viral control (fig. S8). Thus, DP2 antagonists and DP1 agonists may serve as novel antiviral strategies for the treatment of RSV bronchiolitis.

Despite the prevailing view that mast cells are the primary source of PGD2 (*38*), in both our in vitro and in vivo model systems, we observed large numbers of h-PGDS immunoreactive AECs in response to virus infection, with a concomitant production of PGD2. In the AEC cultures, this endogenously produced PGD2 appeared to preferentially activate DP2; treatment with a specific DP1 agonist or DP2 antagonist led to increased IFN-λ (IL-28A) and attenuated viral replication. The same phenotype was observed in the in vivo model of respiratory infection; treatment with the DP1 agonist or DP2 antagonist increased IFN-λ (IL-28A) production, accelerating viral clearance and decreasing immunopathology. The latter may reflect a direct effect of IFN-λ (IL-28A), because the activation of the type III IFN receptor on neutrophils can suppress a proinflammatory gene signature in response to influenza A virus infection (*39*).

DP2 antagonists have been developed for the treatment of allergic indications (*40*). We previously identified that allergen-induced IL-33 release during acute PVM infection increases the severity of viral bronchiolitis in mice by suppressing plasmacytoid DC–mediated antiviral immunity (*19*). Here, our findings suggest that IL-33 might also dampen antiviral immunity via the induction of h-PGDS expression and downstream PGD2 production. Others have shown that DP2 blockade decreases RSV-induced ocular inflammation using a mouse model of allergic conjunctivitis (*41*). However, the investigators did not assess viral load or elucidate the mechanism by which DP2 antagonism was protective. In our preclinical model, dual DP1 and DP2 antagonism ablated the beneficial effects of DP2 antagonism, implicating a critical role for PGD2/DP1 signaling, consistent with the protective phenotype conferred by treatment with the DP1 agonist. We resolved that, consequent to the antagonism of DP2, the preferential activation of

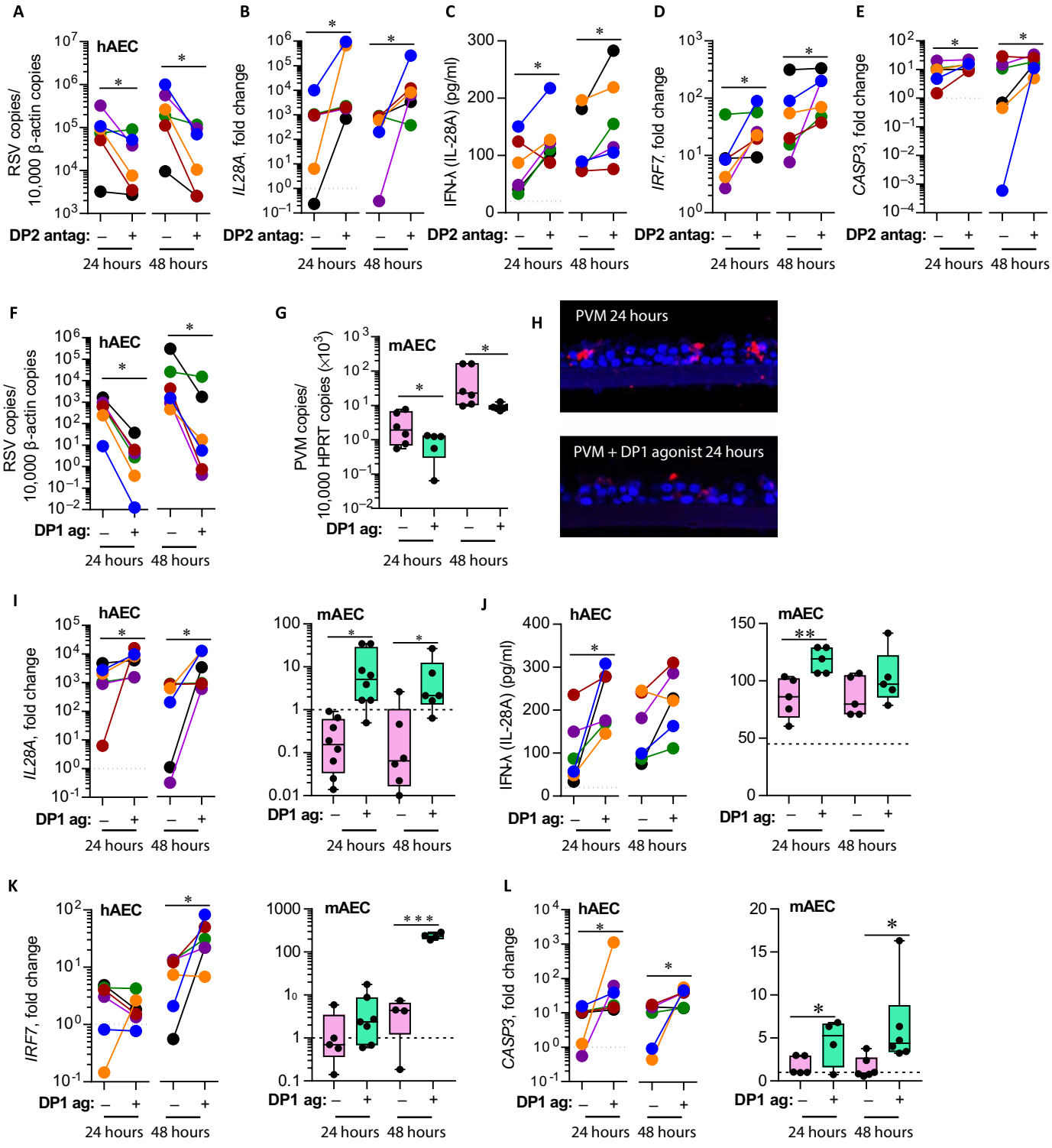


**Fig. 7. DP2 antagonism or DP1 activation of AECs promotes IFN-λ expression to alleviate viral burden.** (**A**) hAECs were preincubated with 50 nM DP2 antagonist (AM156) before infection with RSV (MOI, 1). Viral copies were assessed by qPCR at 24 and 48 hours after infection. (**B**) *IL28A* gene expression and (**C**) IFN-λ (IL-28A) protein expression. (**D**) *IRF7* and (**E**) *CASP3* gene expression. (**F**) hAECs or mouse AECs (mAECs) were infected with RSV or PVM (MOI, 1), respectively. Cells were preincubated with 100 nM DP1 agonist (BW245C). Viral copies were assessed by qPCR at 24 and 48 hours after RSV infection. (**G**) PVM viral copies and (**H**) G protein expression in mAECs differentiated at the air-liquid interface. (**I**) *IL28A* gene expression in hAECs (left) and mAECs (right). (**J**) IFN-λ (hIL-28A or mIL-28A/B) protein expression. (**K**) *IRF7* gene expression. (**L**) *CASP3* gene expression. Box-and-whisker plots show quartiles (boxes) and range (whiskers), and data are representative of three experiments ($n = 6$ individual patients or mice in duplicate), analyzed by Wilcoxon or Mann-Whitney test. *$P < 0.05$, **$P < 0.01$, and ***$P < 0.001$. Dashed lines represent uninfected controls.

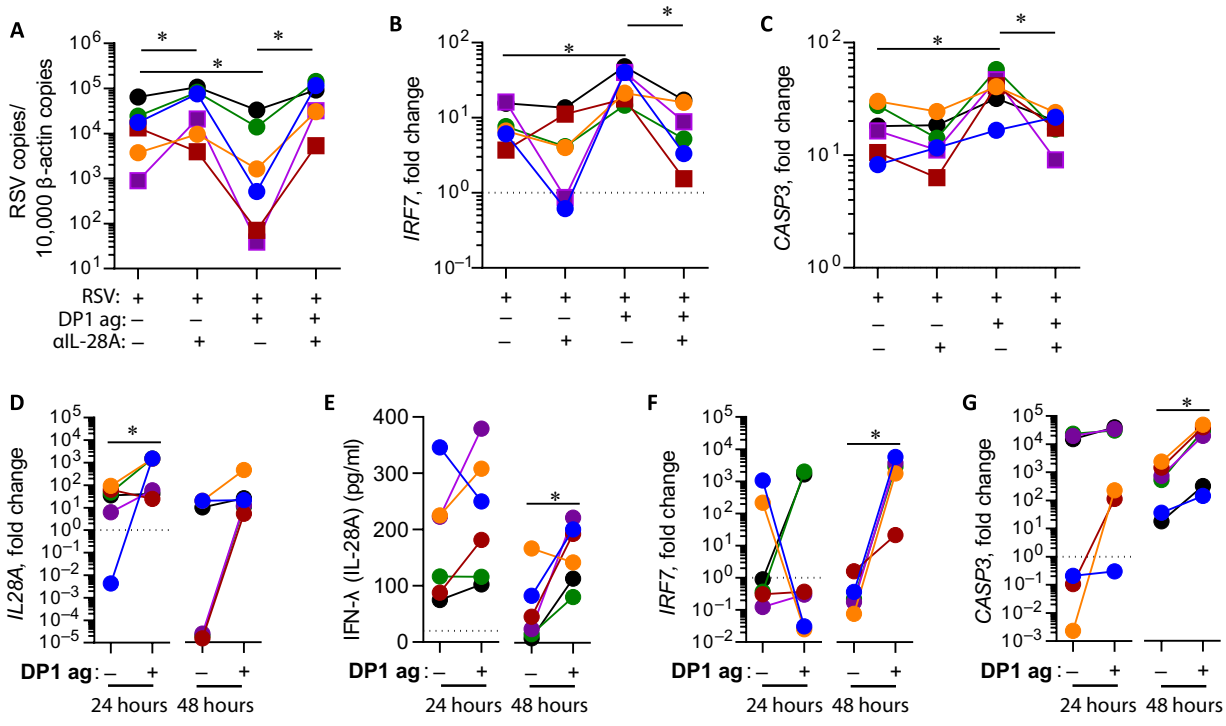


**Fig. 8. DP1 activation of AECs promotes IFN-λ expression.** (**A**) hAECs were preincubated with anti–IL-28A before infection (MOI, 1) ± DP1 agonist. Viral copies and (**B**) *IRF7* gene and (**C**) *CASP3* gene expression were assessed by qPCR at 48 hours. (**D**) hAECs were treated with polyI:C ± DP1 agonist. *IL28A* gene expression, (**E**) IFN-λ (IL-28A) protein expression, and (**F**) *IRF7* and (**G**) *CASP3* gene expression. Box-and-whisker plots show quartiles (boxes) and range (whiskers), and data are representative of three experiments ($n = 6$ individual patients per mice in duplicate), analyzed by Wilcoxon or Mann-Whitney test. *$P < 0.05$. Dashed lines represent uninfected controls.

DP1 increases the production of IFN-λ, decreases viral burden, and ameliorates the severity of bronchiolitis in early life.

In response to respiratory virus infection, cultured AECs from asthmatic subjects produce less type I and type III IFN as compared to healthy controls (*42*, *43*). This phenotype has been reproduced by other laboratories (*29*, *44*), although not universally (*45*, *46*). Our in vivo study suggested that leukocyte-derived and then, later in the infection, epithelial-derived PGD2 controls the production of IFN-λ (IL-28A), implicating a critical role for PGD2 and, more specifically, the activation of DP1 or DP2 in regulating epithelial host defense. Mechanistically, we demonstrated that IFN-λ (IL-28A) promoted ISG expression in the cultured hAECs, including the expression of caspase-3, to promote viral control (although, notably, *Casp3* expression did not always correlate with IFN expression, possibly because viral load is a key determinant). These pathways were reproduced in the in vivo mouse model, where, notably, (i) DP1 activation increased IFN-λ (IL-28A) production at 5 dpi in PVM-infected mice independently of an inhibitory effect driven by DP2 signaling, and (ii) the beneficial effects of DP2 antagonism were abrogated in the presence of anti–IL-28A. Thus, DP1 signaling positively regulates the expression of IFN-λ. This effect (both in vivo and in vitro) appeared to be independent of IL-4 and IL-13, which have been shown to suppress type I and type III IFNs (*20*, *29*). Critically, DP1 activation also enhanced the antiviral response of hAECs stimulated with the viral mimetic double-stranded DNA polyI:C, suggesting that DP1 agonists may offer benefit for the treatment of RSV bronchiolitis and other viral infections.

Severe viral bronchiolitis and allergic sensitization are independent risk factors for asthma onset; however, this risk is magnified in young children who are both sensitized and experience severe and/or frequent lower respiratory infections (*17*, *18*). Whether viral bronchiolitis is causal for asthma remains contentious; however, in one clinical study, it was estimated that if RSV bronchiolitis were causal, then its elimination could prevent up to 13% of asthma cases (*15*). To simulate the human epidemiology, we previously developed a preclinical model whereby virus- and allergen-coexposed neonatal mice are predisposed to develop asthma-like pathologies upon secondary virus and allergen exposure in later life (*19*). Here, we took advantage of this model and demonstrated that DP2 antagonism in early life alone decreased the onset of type 2 immunity and airway remodeling in infancy and, moreover, was sufficient to prevent PVM/CRE-induced progression to an asthma-like pathology in later life. Thus, DP2 antagonism acted as an effective primary preventative when used in early life. In addition to RSV, rhinovirus infections can also cause bronchiolitis, and in sensitized individuals, rhinovirus infections are associated with greater risk of asthma development (*16*). It is probable that PGD2 also plays a pathogenic role in this setting, because rhinovirus infection of cultured hAECs has been shown to induce PGD2 production (*47*).

Recent phase 2a trials of small-molecule DP2 antagonists are encouraging, demonstrating improvements in both eosinophil numbers and lung function, even in patients with severe asthma receiving oral corticosteroids (*12*, *13*). Although these drugs are known to decrease type 2 inflammation via antagonism of PGD2/DP2, our findings show that these drugs may also promote this outcome by increasing DP1 activation, which (i) directly attenuates ILC2 proliferation and type 2 cytokine production and (ii) increases IFN-λ expression, a negative regulator of type 2 cytokine production. Perhaps more importantly,

our findings demonstrate that DP2 antagonists, in addition to decreasing type 2 inflammation, would also boost antiviral immunity and thus lower the incidence of virally-triggered exacerbations. In light of the detrimental effects of corticosteroids on antiviral immunity, clinical studies are now required to evaluate whether treatment with DP2 antagonists will allow for steroid-sparing, as has been shown with biologics targeting IL-4R and IL-5 (*48*, *49*).

Increased ASM mass is a hallmark feature of asthma that is now recognized to develop in young children, predating asthma diagnosis (*30*). Strikingly, we observed that DP2 blockade prevented the aberrant ASM growth during bronchiolitis in early life. This intervention was sufficient to prevent ASM growth upon secondary virus and allergen exposure in later life, although whether this relates to an ASM intrinsic or extrinsic mechanism remains to be determined. PGD2 is well established as a potent bronchoconstrictor (*3*, *4*); however, in this study, we identified that PGD2 is also an effective mitogen of primary mouse ASM cells. This response to PGD2 was mediated via DP2, and DP1 agonism (both in vivo and in vitro) once again served to counter the pathogenic effects mediated by PGD2/DP2 signaling.

Previous studies have demonstrated that DP1 and DP2 activation elicit opposing effects on the development of $T_H2$ immunity. For example, DP2 activation promotes chemotaxis and the activation of $T_H2$ effector cells, whereas DP1 agonists promote tolerogenic DCs and the differentiation of regulatory T cells (*6*, *9*). Here, we extend this paradigm to show that DP2 and DP1 activation exert opposing effects on ASM cell proliferation and AEC antiviral cytokine production. Despite the fact that PGD2 binds to both receptors with similar affinity (*50*), endogenously produced PGD2 preferentially activated DP2 in both the in vitro and in vivo model, and thus, the production of PGD2 during RSV infection was deleterious. The differential distribution of the two receptors might underlie this effect; for example, DP2 is highly expressed on type 2 effector cells (*5*, *6*) and is further up-regulated during inflammation (*51*); however, we found that both receptors, as measured by qPCR, were expressed at the same level on AECs and ASM cells. Note that many of the metabolites of PGD2, including DK-PGD2, $\Delta^{12}$PGD2, and $\Delta^{12}$PGJ2 (*52*–*54*), are highly selective for DP2 and can suppress antiviral immunity (*55*), and thus, we speculate that the dominant DP2 phenotype is underpinned by these compounds. Another limitation of our study is that we have yet to resolve the molecular mechanism by which DP1 signaling increases the production of IFN-λ.

In conclusion, we show that PGD2 production is elevated in nasopharyngeal samples in young infants hospitalized with RSV bronchiolitis. Using species-specific pneumoviruses in in vivo and in vitro model systems, we revealed that PGD2 contributes to disease severity by suppressing antiviral immunity and promoting type 2 inflammation. DP2 antagonism reversed the deleterious effects of PGD2 by favoring the activation of DP1. Accordingly, DP2 antagonists or DP1 agonists may prove useful for the treatment of viral bronchiolitis, viral-triggered exacerbations of asthma, and potentially other indications where viruses contribute to disease pathogenesis.

## MATERIALS AND METHODS

### Study design

The aim of this study was to understand the role of PGD2 in viral bronchiolitis. We used primary hAECs, nasopharyngeal samples from infants with RSV bronchiolitis, and a mouse model of severe viral bronchiolitis. Specific DP1 and DP2 antagonists and agonists were used in vivo and in vitro to implicate these receptors to phenotypic outcomes. Human primary AECs were obtained from Lonza ($n = 6$ patients). Nasopharyngeal samples from young infants hospitalized with RSV bronchiolitis were compared to healthy controls. The sample size in this study was based on the number of infants presenting to the hospital with RSV bronchiolitis (during the RSV season) with samples that we were able to methyloximate in time to stabilize PGD2. For in vivo studies, we used a neonatal model of severe viral bronchiolitis. The basic experimental design of animal experiments used in this study is depicted in Fig. 1A, and intervention study designs are depicted in Figs. 3A, 5A, and 6A. Litter sizes were standardized 1 day after birth, and mice were randomly assigned to treatment groups. The sample size of the viral bronchiolitis and subsequent asthma model experiments was based on our previous experience with this animal model (*19*, *21*). The investigators were not blinded to treatments; however, histology was quantified blinded. Figure legends include details of replicate experiments. No data were excluded from this study. Primary data are located in table S3. All animal studies were approved by the University of Queensland Animal Ethics Committee (protocols 209/13 and 194/16). Ethical approval for collecting patient samples was obtained from the ethics committee at the Princess Margaret Hospital for Children (protocol 1761EP).

### Virus and allergen exposure and drug administration

Specific pathogen-free BALB/c mice (obtained from the Animal Resources Centre and bred at the University of Queensland) were inoculated (intranasal route) at 7 days of age with 1 PFU of PVM (strain J3666) (*19*, *56*) or vehicle [Dulbecco's modified Eagle's medium + 10% fetal calf serum (FCS)] under light isoflurane–induced anesthesia. Three days later, the mice were exposed (intranasal route) to 1 μg of CRE (GREER Laboratories) or vehicle [phosphate-buffered saline (PBS)] and euthanized at the times indicated (Fig. 1). In some experiments, mice were infected with PVM and then exposed (intranasal route) to exogenous IL-33 (0.5 μg/kg) daily at 3 to 5 dpi, or PVM/CRE-coexposed mice were treated with anti–IL-33 or isotype control (200 μg) at 4, 6, and 8 dpi (*19*). To progress disease to an asthma-like phenotype, mice inoculated in early life with PVM and CRE were reinfected 6 weeks later with PVM (20 PFU) and exposed to CRE at 45, 49, 56, and 63 dpi (Fig. 4).

To antagonize DP1 and/or DP2, mice were treated (oral gavage) daily at 3 to 9 dpi with the DP2 antagonist AM156 (*57*) (synthesized by G. Painter and K. Johnston of the Ferrier Institute, Victoria University, Wellington, New Zealand) and/or the DP1 antagonist MK-0524 (Cayman Chemical) at 10 and 5 mg/kg, respectively, as previously described (*57*, *58*). To activate DP1 or DP2, mice were treated (intranasal route) daily at 3 to 9 dpi with the DP1 agonist (1 mg/kg; BW 245C, Cayman Chemical) or the DP2 agonist (1 mg/kg; 15*R*-methyl-PGD2, Cayman Chemical), doses at which the agonists are selective for the respective receptor (*59*, *60*). Exogenous PGD2 was used at 5 μg/kg (Cayman Chemical). In some experiments, mice were treated with anti–IL-28A (1 mg/kg; R&D Systems) or soluble IL-13Rα2 fusion protein (40 mg/kg; Pfizer).

### Airway epithelial cell culture

Human bronchial AECs were obtained from healthy pediatric donors (Lonza; table S1). Cells were grown in steroid-supplemented bronchial epithelial growth medium (Lonza) until 75% confluent, and then culture medium was replaced with steroid-free medium 24 hours before infection with RSV. Primary cells were incubated with RSVA2

(MOI, 1) for 2 hours at 37°C before the cells were washed three times with PBS and cultured with steroid-free culture medium. Cell supernatant was collected 24 and 48 hours after infection and stabilized for PGD2 detection (as detailed below). The cells were stored in TRI Reagent (Ambion) for RNA extraction or fixed with 10% formalin for 10 min, washed three times with PBS, and then stained for h-PGDS (details below).

Primary mAECs were isolated as described previously (*61*). Cells were grown submerged on transwell inserts (BD Falcon) until confluent before the apical medium was lifted to create an air-liquid interface. Once differentiated (as determined by ciliation and transepithelial electrical resistance of >1000), the cells were inoculated with PVM (MOI, 1), washed at 8 hours, and then collected for RNA harvesting in TRI Reagent at 24 and 48 hours after infection. Basolateral supernatants were stored at −80°C for protein analysis.

In some experiments, the cells were treated for 30 min before infection with a DP2 antagonist (50 nM; AM156), a DP1 agonist (100 nM; BW 245C), a DP2 agonist [15(*R*)-15-methyl-PGD2; 10 nM], anti–IL-28A (1 μg/ml; R&D Systems), or anti–IL-4 (0.5 μg/ml) and anti–IL-13 (0.5 μg/ml) (PeproTech). To mimic viral infection, cells were treated with polyI:C (1 μg/ml; Sigma-Aldrich).

### Bronchiolitis subjects

Children were admitted to the hospital with viral bronchiolitis (details in Fig. 2D). Healthy subjects were recruited from the surgical ward and did not have bronchiolitis or other respiratory complications. Consent was obtained from parents and viral species detected using quantitative real-time PCR. Nasal swab sampling was performed by a single investigator and involved rotating a soft flocked nasal swab around the nostril. Swabs were collected and spun to obtain a cell-free supernatant, which was immediately stabilized for PGD2 detection, as described below.

### PGD2 stabilization and detection

Briefly, lung lobes were homogenized, or supernatant was collected and then liquid-extracted using acetone. Samples were spun and washed twice and then evaporated to dryness under a stream of compressed air (about 2 min). All samples (lung samples, nasal swabs, and cell supernatant) were methyloximated to stabilize PGD2, and the assay was run as per the manufacturer's instructions. A PGD2-MOX Express ELISA kit (mouse) or a PGD2-MOX ELISA kit (human samples) was used to detect PGD2 production (Cayman Chemical). According to the manufacturer, cross-reactivity with similar molecules (for example, PGF2α or prostaglandin E2) is <1%.

### ASM culture

Mouse tracheal smooth muscle cells from naïve, 21-day-old mice were isolated using 0.15% pronase at 4°C overnight, as described previously (*62*). Cells were passaged up to four times before use in proliferation assays. ASM cells were dyed with V450 proliferation dye (eBioscience), washed, and plated overnight in 10% FCS-supplemented media. Cells were then serum-starved overnight, before stimulation with PGD2, a DP1 agonist (120 nM, BW 245C), or a DP2 antagonist (10 pM, 15*R*-methyl-PGD2) for 4 days. Proliferation (dilution of V450 dye) was measured with an LSRFortessa X-20 (BD Biosciences) and normalized to maximum (10% FCS) and minimum (1% FCS) proliferation.

### ILC2 culture

ILC2s ($CD2^-$, $CD3^-$, $CD11c^-$, $CD11b^-$, $B220^-$, $Gr\text{-}1^-$, $CD25^+$, $ST\text{-}2^+$, and $CD90.2^+$) were FACS-sorted (>95% purity) as described previously (*19*) from the lungs of PVM/CRE-coexposed mice at 10 dpi. Cells were stained with CFSE and then cultured with IL-2 (30 ng/ml) and stimulated with IL-33 (30 ng/ml) or PGD2 (100 ng/ml). In some experiments, the cells were treated with AM156 (100 nM), IFN-λ (100 ng/ml), or BW245C (100 nM). Supernatant was collected after 96 hours, and cell proliferation (CFSE dilution) and/or apoptosis (annexin 5 expression) was measured by flow cytometry.

### Statistical analyses

GraphPad Prism version 5.0 software was used for all statistical analyses. A Student's *t* test, one-way ANOVA with a Tukey's post hoc test, or two-way ANOVA with a Sidak post hoc test was applied as appropriate. $P < 0.05$ was considered statistically significant.

## SUPPLEMENTARY MATERIALS

www.sciencetranslationalmedicine.org/cgi/content/full/10/440/eaao0052/DC1

Materials and Methods

Fig. S1. h-PGDS expression.

Fig. S2. Effect of DP2 antagonism on antiviral immune cells.

Fig. S3. Effect of DP2 antagonism on type 2 inflammation.

Fig. S4. Effect of DP2 antagonism is not mediated by IL-13.

Fig. S5. Effect of DP1 and/or DP2 antagonism on antiviral cytokines.

Fig. S6. Effect of DP1 and/or DP2 agonism on antiviral cytokines.

Fig. S7. Effect of anti-$T_H2$, DP1-alone or $RSV^+$DP2 agonism in hAECs.

Fig. S8. A simplified schematic of the proposed mechanisms by which PGD2 suppresses or promotes antiviral immunity.

Table S1. hAEC donor characteristics.

Table S2. Oligonucleotide sequences used in this study.

Table S3. Primary data from this study.

References (*63*–*65*)

## REFERENCES AND NOTES


1. B. N. Lambrecht, H. Hammad, The immunology of asthma. *Nat. Immunol.* **16**, 45–56 (2015).
2. G. F. Sonnenberg, D. Artis, Innate lymphoid cells in the initiation, regulation and resolution of inflammation. *Nat. Med.* **21**, 698–708 (2015).
3. J. J. Murray, A. B. Tonnel, A. R. Brash, L. J. Roberts II, P. Gosset, R. Workman, A. Capron, J. A. Oates, Release of prostaglandin $D_2$ into human airways during acute antigen challenge. *N. Engl. J. Med.* **315**, 800–804 (1986).
4. R. W. Fuller, C. M. S. Dixon, C. T. Dollery, P. J. Barnes, Prostaglandin $D_2$ potentiates airway responsiveness to histamine and methacholine. *Am. Rev. Respir. Dis.* **133**, 252–254 (1986).
5. L. Xue, M. Salimi, I. Panse, J. M. Mjösberg, A. N. J. McKenzie, H. Spits, P. Klenerman, G. Ogg, Prostaglandin $D_2$ activates group 2 innate lymphoid cells through chemoattractant receptor-homologous molecule expressed on $T_H2$ cells. *J. Allergy Clin. Immunol.* **133**, 1184–1194.e7 (2014).
6. H. Hirai, K. Tanaka, O. Yoshie, K. Ogawa, K. Kenmotsu, Y. Takamori, M. Ichimasa, K. Sugamura, M. Nakamura, S. Takano, K. Nagata, Prostaglandin $D_2$ selectively induces chemotaxis in T helper type 2 cells, eosinophils, and basophils via seven-transmembrane receptor CRTH2. *J. Exp. Med.* **193**, 255–261 (2001).
7. P. J. Barnes, New therapies for asthma: Is there any progress? *Trends Pharmacol. Sci.* **31**, 335–343 (2010).
8. P. Gosset, F. Bureau, V. Angeli, M. Pichavant, C. Faveeuw, A.-B. Tonnel, F. Trottein, Prostaglandin $D_2$ affects the maturation of human monocyte-derived dendritic cells: Consequence on the polarization of naive Th cells. *J. Immunol.* **170**, 4943–4952 (2003).
9. H. Hammad, M. Kool, T. Soullié, S. Narumiya, F. Trottein, H. C. Hoogsteden, B. N. Lambrecht, Activation of the D prostanoid 1 receptor suppresses asthma by modulation of lung dendritic cell function and induction of regulatory T cells. *J. Exp. Med.* **204**, 357–367 (2007).
10. G. Bain, D. S. Lorrain, K. J. Stebbins, A. R. Broadhead, A. M. Santini, P. Prodanovich, J. Darlington, C. D. King, C. Lee, C. Baccei, B. Stearns, Y. Troung, J. H. Hutchinson, P. Prasit, J. F. Evans, Pharmacology of AM211, a potent and selective prostaglandin $D_2$ receptor type 2 antagonist that is active in animal models of allergic inflammation. *J. Pharmacol. Exp. Ther.* **338**, 290–301 (2011).
11. K. J. Stebbins, A. R. Broadhead, L. D. Correa, J. M. Scott, Y. P. Truong, B. A. Stearns, J. H. Hutchinson, P. Prasit, J. F. Evans, D. S. Lorrain, Therapeutic efficacy of AM156, a novel prostanoid $DP_2$ receptor antagonist, in murine models of allergic rhinitis and house dust mite-induced pulmonary inflammation. *Eur. J. Pharmacol.* **638**, 142–149 (2010).

12. Z. Diamant, P. N. Sidharta, D. Singh, B. J. O'Connor, R. Zuiker, B. R. Leaker, M. Silkey, J. Dingemanse, Setipiprant, a selective CRTH2 antagonist, reduces allergen-induced airway responses in allergic asthmatics. *Clin. Exp. Allergy* **44**, 1044–1052 (2014).
13. S. Gonem, R. Berair, A. Singapuri, R. Hartley, M. F. M. Laurencin, G. Bacher, B. Holzhauer, M. Bourne, V. Mistry, I. D. Pavord, A. H. Mansur, A. J. Wardlaw, S. H. Siddiqui, R. A. Kay, C. E. Brightling, Fevipiprant, a prostaglandin D2 receptor 2 antagonist, in patients with persistent eosinophilic asthma: A single-centre, randomised, double-blind, parallel-group, placebo-controlled trial. *Lancet Respir. Med.* **4**, 699–707 (2016).
14. W. W. Busse, S. E. Wenzel, E. O. Meltzer, E. M. Kerwin, M. C. Liu, N. Zhang, Y. Chon, A. L. Budelsky, J. Lin, S. L. Lin, Safety and efficacy of the prostaglandin D2 receptor antagonist AMG 853 in asthmatic patients. *J. Allergy Clin. Immunol.* **131**, 339–345 (2013).
15. K. M. James, T. Gebretsadik, G. J. Escobar, P. Wu, K. N. Carroll, S. X. Li, E. M. Walsh, E. F. Mitchel, C. D. Sloan, T. V. Hartert, Risk of childhood asthma following infant bronchiolitis during the respiratory syncytial virus season. *J. Allergy Clin. Immunol.* **132**, 227–229 (2013).
16. D. J. Jackson, R. E. Gangnon, M. D. Evans, K. A. Roberg, E. L. Anderson, T. E. Pappas, M. C. Printz, W.-M. Lee, P. A. Shult, E. Reisdorf, K. T. Carlson-Dakes, L. P. Salazar, D. F. DaSilva, C. J. Tisler, J. E. Gern, R. F. Lemanske Jr., Wheezing rhinovirus illnesses in early life predict asthma development in high-risk children. *Am. J. Respir. Crit. Care Med.* **178**, 667–672 (2008).
17. P. G. Holt, J. Rowe, M. Kusel, F. Parsons, E. M. Hollams, A. Bosco, K. McKenna, L. Subrata, N. de Klerk, M. Serralha, B. J. Holt, G. Zhang, R. Loh, S. Ahlstedt, P. D. Sly, Toward improved prediction of risk for atopy and asthma among preschoolers: A prospective cohort study. *J. Allergy Clin. Immunol.* **125**, 653–659.e7 (2010).
18. D. J. Jackson, M. D. Evans, R. E. Gangnon, C. J. Tisler, T. E. Pappas, W.-M. Lee, J. E. Gern, R. F. Lemanske Jr., Evidence for a causal relationship between allergic sensitization and rhinovirus wheezing in early life. *Am. J. Respir. Crit. Care Med.* **185**, 281–285 (2012).
19. J. P. Lynch, R. B. Werder, J. Simpson, Z. Loh, V. Zhang, A. Haque, K. Spann, P. D. Sly, S. B. Mazzone, J. W. Upham, S. Phipps, Aeroallergen-induced IL-33 predisposes to respiratory virus–induced asthma by dampening antiviral immunity. *J. Allergy Clin. Immunol.* **138**, 1326–1337 (2016).
20. M. Contoli, K. Ito, A. Padovani, D. Poletti, B. Marku, M. R. Edwards, L. A. Stanciu, G. Gnesini, A. Pastore, A. Spanevello, P. Morelli, S. L. Johnston, G. Caramori, A. Papi, $T_H2$ cytokines impair innate immune responses to rhinovirus in respiratory epithelial cells. *Allergy* **70**, 910–920 (2015).
21. R. B. Werder, V. Z. Zhang, J. P. Lynch, N. Snape, J. W. Upham, K. Spann, S. Phipps, Chronic IL-33 expression predisposes to virus-induced asthma exacerbations by increasing type 2 inflammation and dampening antiviral immunity. *J. Allergy Clin. Immunol.* 10.1016/j.jaci.2017.07.051(2017).
22. A. S. Feldman, Y. He, M. L. Moore, M. B. Hershenson, T. V. Hartert, Toward primary prevention of asthma. Reviewing the evidence for early-life respiratory viral infections as modifiable risk factors to prevent childhood asthma. *Am. J. Respir. Crit. Care Med.* **191**, 34–44 (2015).
23. Y. Kanaoka, Y. Urade, Hematopoietic prostaglandin D synthase. *Prostaglandins Leukot. Essent. Fatty Acids* **69**, 163–167 (2003).
24. Y. Urade, O. Hayaishi, Biochemical, structural, genetic, physiological, and pathophysiological features of lipocalin-type prostaglandin D synthase. *Biochim. Biophys. Acta* **1482**, 259–271 (2000).
25. G. M. Levasseur-Acker, M. Molimard, J. Regnard, E. Naline, C. Freche, A. Lockhart, Effect of furosemide on prostaglandin synthesis by human nasal and bronchial epithelial cells in culture. *Am. J. Respir. Cell Mol. Biol.* **10**, 378–383 (1994).
26. A. Roulston, R. C. Marcellus, P. E. Branton, Viruses and apoptosis. *Annu. Rev. Microbiol.* **53**, 577–628 (1999).
27. J. P. Legg, I. R. Hussain, J. A. Warner, S. L. Johnston, J. O. Warner, Type 1 and type 2 cytokine imbalance in acute respiratory syncytial virus bronchiolitis. *Am. J. Respir. Crit. Care Med.* **168**, 633–639 (2003).
28. C. A. Lindemans, J. L. L. Kimpen, B. Luijk, J. Heidema, D. Kanters, C. K. van der Ent, L. Koenderman, Systemic eosinophil response induced by respiratory syncytial virus. *Clin. Exp. Immunol.* **144**, 409–417 (2006).
29. S. Baraldo, M. Contoli, E. Bazzan, G. Turato, A. Padovani, B. Marku, F. Calabrese, G. Caramori, A. Ballarin, D. Snijders, A. Barbato, M. Saetta, A. Papi, Deficient antiviral immune responses in childhood: Distinct roles of atopy and asthma. *J. Allergy Clin. Immunol.* **130**, 1307–1314 (2012).
30. R. O'Reilly, N. Ullmann, S. Irving, C. J. Bossley, S. Sonnappa, J. Zhu, T. Oates, W. Banya, P. K. Jeffery, A. Bush, S. Saglani, Increased airway smooth muscle in preschool wheezers who have asthma at school age. *J. Allergy Clin. Immunol.* **131**, 1024–1032 (2013).
31. I. Ioannidis, F. Ye, B. McNally, M. Willette, E. Flaño, Toll-like receptor expression and induction of type I and type III interferons in primary airway epithelial cells. *J. Virol.* **87**, 3261–3270 (2013).
32. S. C. Buckingham, A. J. Bush, J. P. Devincenzo, Nasal quantity of respiratory syncytical virus correlates with disease severity in hospitalized infants. *Pediatr. Infect. Dis. J.* **19**, 113–117 (2000).
33. R. Nenna, M. Ferrara, A. Nicolai, A. Pierangeli, C. Scagnolari, P. Papoff, G. Antonelli, C. Moretti, F. Midulla, Viral load in infants hospitalized for respiratory syncytial virus bronchiolitis correlates with recurrent wheezing at thirty-six-month follow-up. *Pediatr. Infect. Dis. J.* **34**, 1131–1132 (2015).
34. K. M. Spann, K.-C. Tran, B. Chi, R. L. Rabin, P. L. Collins, Suppression of the induction of alpha, beta, and gamma interferons by the NS1 and NS2 proteins of human respiratory syncytial virus in human epithelial cells and macrophages. *J. Virol.* **78**, 4363–4369 (2004).
35. A. A. Bakre, J. L. Harcourt, L. M. Haynes, L. J. Anderson, R. A. Tripp, The central conserved region (CCR) of respiratory syncytial virus (RSV) G protein modulates host miRNA expression and alters the cellular response to infection. *Vaccines* **5**, E16 (2017).
36. R. Janssen, L. Bont, C. L. E. Siezen, H. M. Hodemaekers, M. J. Ermers, G. Doornbos, R. van't Slot, C. Wijmenga, J. J. Goeman, J. L. L. Kimpen, H. C. van Houwelingen, T. G. Kimman, B. Hoebee, Genetic susceptibility to respiratory syncytial virus bronchiolitis is predominantly associated with innate immune genes. *J. Infect. Dis.* **196**, 826–834 (2007).
37. A. Pasanen, M. K. Karjalainen, L. Bont, E. Piippo-Savolainen, M. Ruotsalainen, E. Goksör, K. Kumawat, H. Hodemaekers, K. Nuolivirta, T. Jartti, G. Wennergren, M. Hallman, M. Rämet, M. Korppi, Genome-wide association study of polymorphisms predisposing to bronchiolitis. *Sci. Rep.* **7**, 41653 (2017).
38. R. C. Benyon, C. Robinson, M. K. Church, Differential release of histamine and eicosanoids from human skin mast cells activated by IgE-dependent and non-immunological stimuli. *Br. J. Pharmacol.* **97**, 898–904 (1989).
39. I. E. Galani, V. Triantafyllia, E.-E. Eleminiadou, O. Koltsida, A. Stavropoulos, M. Manioudaki, D. Thanos, S. E. Doyle, S. V. Kotenko, K. Thanopoulou, E. Andreakos, Interferon-λ mediates non-redundant front-line antiviral protection against influenza virus infection without compromising host fitness. *Immunity* **46**, 875–890.e6 (2017).
40. R. Pettipher, T. T. Hansel, R. Armer, Antagonism of the prostaglandin $D_2$ receptors $DP_1$ and CRTH2 as an approach to treat allergic diseases. *Nat. Rev. Drug Discov.* **6**, 313–325 (2007).
41. K. J. Stebbins, A. R. Broadhead, A. Musiyenko, S. Barik, J. M. Scott, Y. P. Truong, B. A. Stearns, J. H. Hutchinson, P. Prasit, J. F. Evans, D. S. Lorrain, DP2 (CRTH2) antagonism reduces ocular inflammation induced by allergen challenge and respiratory syncytial virus. *Int. Arch. Allergy Immunol.* **157**, 259–268 (2012).
42. M. Contoli, S. D. Message, V. Laza-Stanca, M. R. Edwards, P. A. B. Wark, N. W. Bartlett, T. Kebadze, P. Mallia, L. A. Stanciu, H. L. Parker, L. Slater, A. Lewis-Antes, O. M. Kon, S. T. Holgate, D. E. Davies, S. V. Kotenko, A. Papi, S. L. Johnston, Role of deficient type III interferon-λ production in asthma exacerbations. *Nat. Med.* **12**, 1023–1026 (2006).
43. P. A. B. Wark, S. L. Johnston, F. Bucchieri, R. Powell, S. Puddicombe, V. Laza-Stanca, S. T. Holgate, D. E. Davies, Asthmatic bronchial epithelial cells have a deficient innate immune response to infection with rhinovirus. *J. Exp. Med.* **201**, 937–947 (2005).
44. K. M. Spann, E. Baturcam, J. Schagen, C. Jones, C. P. Straub, F. M. Preston, L. Chen, S. Phipps, P. D. Sly, E. Fantino, Viral and host factors determine innate immune responses in airway epithelial cells from children with wheeze and atopy. *Thorax* **69**, 918–925 (2014).
45. Y. A. Bochkov, K. M. Hanson, S. Keles, R. A. Brockman-Schneider, N. N. Jarjour, J. E. Gern, Rhinovirus-induced modulation of gene expression in bronchial epithelial cells from subjects with asthma. *Mucosal Immunol.* **3**, 69–80 (2010).
46. N. Lopez-Souza, S. Favoreto, H. Wong, T. Ward, S. Yagi, D. Schnurr, W. E. Finkbeiner, G. M. Dolganov, J. H. Widdicombe, H. A. Boushey, P. C. Avila, In vitro susceptibility to rhinovirus infection is greater for bronchial than for nasal airway epithelial cells in human subjects. *J. Allergy Clin. Immunol.* **123**, 1384–1390.e2 (2009).
47. D. Van Ly, A. Faiz, C. Jenkins, B. Crossett, J. L. Black, B. McParland, J. K. Burgess, B. G. G. Oliver, Characterising the mechanism of airway smooth muscle $\beta_2$ adrenoceptor desensitization by rhinovirus infected bronchial epithelial cells. *PLOS ONE* **8**, e56058 (2013).
48. S. Wenzel, L. Ford, D. Pearlman, S. Spector, L. Sher, F. Skobieranda, L. Wang, S. Kirkesseli, R. Rocklin, B. Bock, J. Hamilton, J. E. Ming, A. Radin, N. Stahl, G. D. Yancopoulos, N. Graham, G. Pirozzi Dupilumab in persistent asthma with elevated eosinophil levels. *N. Engl. J. Med.* **368**, 2455–2466 (2013).
49. I. D. Pavord, S. Korn, P. Howarth, E. R. Bleecker, R. Buhl, O. N. Keene, H. Ortega, P. Chanez, Mepolizumab for severe eosinophilic asthma (DREAM): A multicentre, double-blind, placebo-controlled trial. *Lancet* **380**, 651–659 (2012).
50. E. Ricciotti, G. A. FitzGerald, Prostaglandins and inflammation. *Arterioscler. Thromb. Vasc. Biol.* **31**, 986–1000 (2011).
51. M. L. Fajt, S. L. Gelhaus, B. Freeman, C. E. Uvalle, J. B. Trudeau, F. Holguin, S. E. Wenzel, Prostaglandin $D_2$ pathway upregulation: Relation to asthma severity, control, and $T_H2$ inflammation. *J. Allergy Clin. Immunol.* **131**, 1504–1512 (2013).
52. L. Gazi, S. Gyles, J. Rose, S. Lees, C. Allan, L. Xue, R. Jassal, G. Speight, V. Gamble, R. Pettipher, Δ12-Prostaglandin D2 is a potent and selective CRTH2 receptor agonist and causes activation of human eosinophils and $T_H2$ lymphocytes. *Prostaglandins Other Lipid Mediat.* **75**, 153–167 (2005).

53. A. Heinemann, R. Schuligoi, I. Sabroe, A. Hartnell, B. A. Peskar, $\Delta^{12}$-Prostaglandin $J_2$, a plasma metabolite of prostaglandin $D_2$, causes eosinophil mobilization from the bone marrow and primes eosinophils for chemotaxis. *J. Immunol.* **170**, 4752–4758 (2003).
54. R. Schuligoi, R. Schmidt, G. Geisslinger, M. Kollroser, B. A. Peskar, A. Heinemann, PGD2 metabolism in plasma: Kinetics and relationship with bioactivity on DP1 and CRTH2 receptors. *Biochem. Pharmacol.* **74**, 107–117 (2007).
55. R. Arnold, W. König, Peroxisome proliferator-activated receptor-γ agonists inhibit the replication of syncytial virus (RSV) in human lung epithelial cells. *Virology* **350**, 335–346 (2006).
56. S. Davidson, G. Kaiko, Z. Loh, A. Lalwani, V. Zhang, K. Spann, S. Y. Foo, N. Hansbro, S. Uematsu, S. Akira, K. I. Matthaei, H. F. Rosenberg, P. S. Foster, S. Phipps, Plasmacytoid dendritic cells promote host defense against acute pneumovirus infection via the TLR7-MyD88-dependent signaling pathway. *J. Immunol.* **186**, 5938–5948 (2011).
57. K. J. Stebbins, A. R. Broadhead, C. S. Baccei, J. M. Scott, Y. P. Truong, H. Coate, N. S. Stock, A. M. Santini, P. Fagan, P. Prodanovich, G. Bain, B. A. Stearns, C. D. King, J. H. Hutchinson, P. Prasit, J. F. Evans, D. S. Lorrain, Pharmacological blockade of the DP2 receptor inhibits cigarette smoke-induced inflammation, mucus cell metaplasia, and epithelial hyperplasia in the mouse lung. *J. Pharmacol. Exp. Ther.* **332**, 764–775 (2010).
58. K. Cheng, T.-J. Wu, K. K. Wu, C. Sturino, K. Metters, K. Gottesdiener, S. D. Wright, Z. Wang, G. O'Neill, E. Lai, M. G. Waters, Antagonism of the prostaglandin $D_2$ receptor 1 suppresses nicotinic acid-induced vasodilation in mice and humans. *Proc. Natl. Acad. Sci. U.S.A.* **103**, 6682–6687 (2006).
59. K. Kobayashi, Y. Tsubosaka, M. Hori, S. Narumiya, H. Ozaki, T. Murata, Prostaglandin $D_2$-DP signaling promotes endothelial barrier function via the cAMP/PKA/Tiam1/Rac1 pathway. *Arterioscler. Thromb. Vasc. Biol.* **33**, 565–571 (2013).
60. G. Monneret, C. Cossette, S. Gravel, J. Rokach, W. S. Powell, 15*R*-methyl-prostaglandin $D_2$ is a potent and selective CRTH2/$DP_2$ receptor agonist in human eosinophils. *J. Pharmacol. Exp. Ther.* **304**, 349–355 (2003).
61. J. R. Rock, M. W. Onaitis, E. L. Rawlins, Y. Lu, C. P. Clark, Y. Xue, S. H. Randell, B. L. M. Hogan, Basal cells as stem cells of the mouse trachea and human airway epithelium. *Proc. Natl. Acad. Sci.* **106**, 12771–12775 (2009).
62. M. E. Lauer, D. Mukhopadhyay, C. Fulop, C. A. de la Motte, A. K. Majors, V. C. Hascall, Primary murine airway smooth muscle cells exposed to poly(I,C) or tunicamycin synthesize a leukocyte-adhesive hyaluronan matrix. *J. Biol. Chem.* **284**, 5299–5312 (2009).
63. G. E. Kaiko, Z. Loh, K. Spann, J. P. Lynch, A. Lalwani, Z. Zheng, S. Davidson, S. Uematsu, S. Akira, J. Hayball, K. R. Diener, K. J. Baines, J. L. Simpson, P. G. Gibson, P. S. Foster, S. Phipps, Toll-like receptor 7 gene deficiency and early-life *Pneumovirus* infection interact to predispose toward the development of asthma-like pathology in mice. *J. Allergy Clin. Immunol.* **131**, 1331–1339.e10 (2013).
64. J. Arikkatt, M. A. Ullah, K. R. Short, V. Zhang, W. J. Gan, Z. Loh, R. B. Werder, J. Simpson, P. D. Sly, S. B. Mazzone, K. M. Spann, M. A. R. Ferreira, J. W. Upham, M. B. Sukkar, S. Phipps, RAGE deficiency predisposes mice to virus-induced paucigranulocytic asthma. *eLife* **6**, e21199 (2017).
65. E. Baturcam, N. Snape, T. H. Yeo, J. Schagen, E. Thomas, J. Logan, S. Galbraith, N. Collinson, S. Phipps, E. Fantino, P. D. Sly, K. M. Spann, Human metapneumovirus impairs apoptosis of nasal epithelial cells in asthma via HSP70. *J. Innate Immun.* **9**, 52–64 (2017).


**Acknowledgments:** We thank G. Painter and K. Johnston (Ferrier Institute, Victoria University, Wellington, New Zealand) for synthesizing AM156 and U. Buchholz (National Institute of Allergy and Infectious Diseases, NIH) for anti-PVM antibody. **Funding:** This work was supported by an Australian Infectious Disease Research Excellence Award awarded to S.P., J.P.L., and J.W.U.; a National Health and Medical Research Council Development grant awarded to M.L.S. and S.P.; and an Australian Research Council Future Fellowship to S.P. R.B.W. received training in mouse epithelial cell culture in B. Hogan's laboratory (Duke University) facilitated by a University of Queensland Graduate School International Travel Award. **Author contributions:** R.B.W. and S.P. conceived and designed experiments. R.B.W., J.P.L., J.C.S., V.Z., and N.H.H. conducted experiments. M.P. and M.L.E. collected clinical samples. E.F.-B., C.K., M.L.S., J.W.U., and K.S. provided reagents and intellectual input. R.B.W. and S.P. wrote and edited the paper. **Competing interests:** The authors declare that they have no competing interests.

Submitted 5 June 2017
Resubmitted 17 November 2017
Accepted 12 March 2018
Published 9 May 2018
10.1126/scitranslmed.aao0052

**Citation:** R. B. Werder, J. P. Lynch, J. C. Simpson, V. Zhang, N. H. Hodge, M. Poh, E. Forbes-Blom, C. Kulis, M. L. Smythe, J. W. Upham, K. Spann, M. L. Everard, S. Phipps, PGD2/DP2 receptor activation promotes severe viral bronchiolitis by suppressing IFN-λ production. *Sci. Transl. Med.* **10**, eaao0052 (2018).

Science Translational Medicine

# PGD2/DP2 receptor activation promotes severe viral bronchiolitis by suppressing IFN-λ production

Rhiannon B. Werder, Jason P. Lynch, Jennifer C. Simpson, Vivian Zhang, Nick H. Hodge, Matthew Poh, Elizabeth Forbes-Blom, Christina Kulis, Mark L. Smythe, John W. Upham, Kirsten Spann, Mark L. Everard and Simon Phipps

*Sci Transl Med* **10**, eaao0052.
DOI: 10.1126/scitranslmed.aao0052

**RSV gives innate immunity the runaround**

Asthma can be exacerbated by pathogens such as respiratory syncytial virus (RSV); prostaglandin D2 (PGD2) is also important in asthma and is being investigated as a therapeutic target. Werder *et al.* used multiple models to examine how RSV infection may perturb immune responses and influence asthma pathogenesis. Samples from infants with bronchiolitis or primary pediatric epithelial cells infected with RSV had elevated PGD2. Modulating PGD2 signaling in a mouse model of severe bronchiolitis improved antiviral immunity and dampened asthmatic symptoms later in life. This protection was not due to preventing type 2 immunity but instead a restoration of IFN- λ production. Their findings shed light on this host-pathogen interaction and suggest new therapeutic avenues.